International Conference on Renewable Energies and Power Quality (ICREPQ'14)
Cordoba (Spain), 8th to 10th April, 2014
Renewable Energy and Power Quality Journal (RE&PQJ)
ISSN 2172-038 X, No.12, April 2014

# Application of computational fluid dynamics models to aerodynamic design and optimization of wind turbine airfoils

E. Castiñeira-Martínez, I. Solís-Gallego, J. González, J. Fernández Oro,
K. Argüelles Díaz and S. Velarde-Suárez

Área de Mecánica de Fluidos, Departamento de Energía
Universidad de Oviedo
Edificio Departamental Este, Campus Universitario, 33203 Gijón, España (Spain)
Phone: +0034 985 182101, e-mail: sandrav@uniovi.es

**Abstract**

*In this work, the capability of simple numerical models with coarse grids to predict performance coefficients in wind turbine airfoils is explored. A wide range of simulations were performed for a typical wind turbine profile, under the main criteria of design simplicity and low calculation time. The solutions were computed over different mesh sizes using a two-dimensional Reynolds-Average Navier-Stockes (2D-RANS) approach. Spalart-Allmaras, k-ε and k-ω turbulence models were run in the simulations. Lift, drag and momentum coefficients were computed for four incident angles, ranging from -2.5 to 12.5, for each mesh size and turbulence model, comparing them later with experimental data. Results show a useful model which gives a good agreement between numerical and experimental results and can indeed be used as a first approximation previous to a more detailed and expensive study.*

## Key words

Wind turbine airfoils, CFD, 2D-RANS numerical models, turbulence models.

### 1. Introduction.

The state of the art in the development of wind energy conversion systems still poses some questions on the detailed aerodynamic phenomena involved in the flow around the turbine blades, generally governed by quite variable flow conditions and far from the design ones. One of the particular efforts being carried out is based on the use of Computational Fluid Dynamics (CFD) techniques to handle the flow study around the blade airfoils, even in a design stage, previous to the blade construction. For such kind of approach, it is essential a good selection of the main parameters depending on the flow conditions such as the spatial discretization or numerical grid quality, the turbulent closure scheme, the numerical uncertainty, the unsteady treatment, etc.

Several two-dimensional Reynolds-Average Navier-Stockes (2D-RANS) numerical models have been employed in order to predict the aerodynamic performance of wind turbine airfoils with satisfactory results. For instance, Yu et al. [1] have been applying this kind of methodology to study the dynamic stall of an airfoil undergoing sinusoidal pitch oscillations, finding promising results in predicting lift, draft and momentum coefficients. In the cases of real blades at high angles of attack, 2D simulations are known to overpredict drag, due to tip effects in the spanwise distribution of drag. These effects appear to be more pronounced at high incidence angles and can be adequately predicted by a 3D-RANS model (Sorensen et al. [2]). When a full detailed description of the unsteady flow is needed, such as the case of generation and propagation of airfoil noise, large eddy simulation (LES) schemes must be used (Fleig. et al. [3]), with the subsequent higher computational costs.

In this work, the capability of simple numerical models with coarse grids to predict lift and drag

in wind turbine airfoils is explored. The main goal is to develop a simple and fast method which could be employed in the design stage with a low computational cost, in order to select the best alternative between several options, and previous to more detailed and refined simulations which will be needed in further stages of the airfoil development and construction.

The study starts with the CFD numerical study of a typical airfoil geometry used in wind turbines, in order to determine the main criteria to choose the optimum model and numerical parameters, depending on the flow conditions. The study covers the following two main aspects: sensitivity study of the developed computational grid and verification of the better turbulence model to capture the main physical phenomena. In order to contrast the obtained numerical results, the experimental public database of the National Renewable Energy Laboratory (NREL) at Golden, Colorado, USA (Selig et al. [4]) has been considered.

## 2. Methodology

The research begins with the numerical study of a typical airfoil geometry used in wind turbines. For all the cases presented in this study, a FX 63-137 airfoil model was used. Simulations were run combining different parameters, while some of them have been maintained constant such as the incident velocity, computed for a Reynolds number of 350,000 based on the airfoil chord length.

Three parameters were modified: the number of mesh cells, the incident angle of the flow and the turbulence model employed in the simulation. For the sake of comparison, the numerical results achieved were validated with the experimental public database of the NREL (National Renewable Energy Laboratory) at Golden, Colorado, USA (Seling et al. [4]).

### *2.1. Geometry and mesh generation.*

GAMBIT meshing software was used for geometry and mesh generation. This software is associated with Fluent, where later simulations were made. Four mesh densities were created to avoid high skewed elements: a coarse mesh with 2,992 cells, a middle density mesh with 12,451 cells, a high-density mesh with 48,780 cells and one extra mesh for the k-ω SST case with 111,105 cells. In the following, a simple nomenclature is used to refer the different meshes, named G1, G2, G3 and G4, respectively. The purpose of the chosen shape is to create a meshing that is adapted to the geometry from a simple and effective way as shown in Fig.1. However, for the finest meshes it was necessary to make some changes in the geometry of the mesh to keep the stability in the simulations.

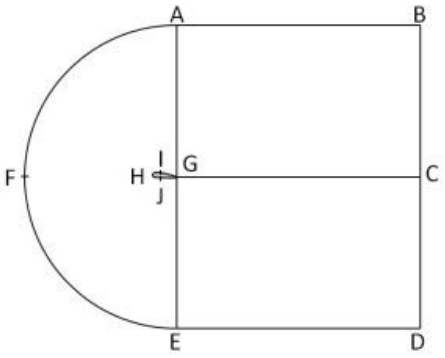


**Fig. 1.** Simple scheme of the geometry of the mesh for coarse and middle mesh.

In Fig. 2, a detail of the middle density mesh is shown, allowing a better appreciation of the airfoil and the geometry of the mesh around it.

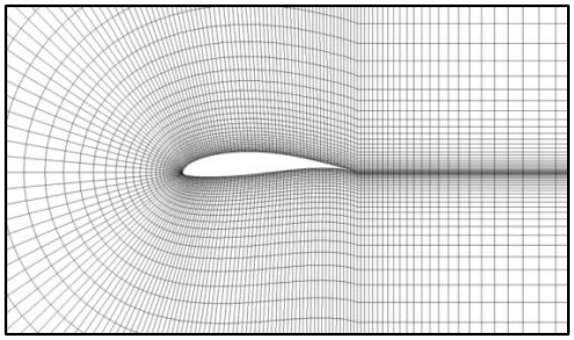

**Fig. 2.** Detail of middle mesh (G2).

### *2.2. Incident angles.*

In this paper, four different incident angles were considered for the simulations: -2.5°, 2.5°, 7.5° and 12.5°, as representative for negative, low, medium and high angles. These have been selected owing to its distribution along the experimental curve, enabling a wide range of results, without excessively increasing the calculation time, which is very important in this study.

*2.3 Turbulence models.*

Simulations were carried out for three different turbulence models: Spalart-Allmaras, k-ε and k-ω using the commercial CFD code, ANSYS FLUENT.

Default constants provided by the program were used for the k-ε and the Spalart-Allmaras models. In particular, the k-ε model employed here is the ReNormalization Group (RNG), a variant of the standard. Variations in the wall functions have been also conducted, running simulations with Standard Wall Functions (SWF) and Enhanded Wall Treatment (EWT).

Finally, initials parameters (k and ω) calculated as exposed by Sorensen et al. [2] and using NREL experimental values were used for the k-ω model. For this model, two variations were conducted. Firstly, the simulations were run with the standard model and later the k-ω SST model of Menter was used, included in this latter the option of transient flows.

It is worth noting that a convergence standard of $10^{-6}$ to the residual parameters was employed.

A Semi Implicit Method for Pressure Linked Equations (SIMPLE) algorithm was applied to enforce the pressure-velocity coupling for the three models and the spatial derivatives are discretized using a second order upwind approach.

In Table 1 the pressure interpolation schemes employed are summarized.

**Table 1.** Pressure interpolation schemes used for each mesh and model.

| S-A | | k-ε | | k-ω |
|---|---|---|---|---|
| **G1,G2** | **G3** | **G1,G2** | **G3** | **G1,G2, G3,G4** |
| PRESTO! | Second Order | Second Order | Standard | Standard |

*2.4 Estimation of errors*

Dimensionless coefficients obtained numerically are compared to the experimental data provided by the bibliography, calculating the average error for the whole range of incident angles considered. As only the simulation of four angles has been performed, the most rational procedure to obtain an estimation of the error is to obtain from the experimental distribution the exact values for each of the simulated angles through a polynomic equation of the tendency line. Afterwards, the global average error is found with equation [1] .

$$R_{global} = \frac{1}{N}\sum_{i=1}^{N}\frac{|C_i^{exp} - C_i^{num}|}{|C_i^{exp}|} \quad [1]$$

where $R_{global}$ is the average error for a specific mesh size and turbulence model, $N$ is the total number of incident angles for which this calculation is made, $C_i^{exp}$ is the appropriate coefficient (lift, drag or momentum) obtained of the experimental study and $C_i^{num}$ is the coefficient obtained by numerical simulation.

**3. Results and discussion**

*3.1 Spalart-Allmaras turbulence model.*

The graphs shown in Fig. 3 correspond to this one-equation turbulence model. The evolution of the lift coefficient presents a notable agreement with the experimental data, even in the case of coarse meshes. As can be seen, results with G2 appear to be the closest to the reference data, while G3, supposed to be closer to the reference values, has a similar behaviour to G1. That could be because the third grid involves an excessive amount of near wall cells for a Spalart-Allmaras turbulence model, as this model does not include any wall treatment.

On the other hand, an accurate estimation of the drag coefficent is more difficult to obtain by numerical simulation, and resulting values are usually overpredicted regarding to experimental data. Overall results appear to improve with the increase of number of cells.

The momentum coefficient is in perfect correspondence with the experimental curve for low angles of attack, deviating gradually with an increasing of the angle of attack.

*3.2. k-ε turbulence model.*

For this model, the graphs are plotted in Fig. 4. The lift coefficient shows an accurate prediction of the values and the tendencies, especially using medium and refined grids, reporting the best values with high incident angles with the

enhanced wall treatment (EWT) model. For this turbulence model, the drag coefficient values are excessively away from the experimental curve in all type of meshes and conditions, thus pointing out that this is not a good model to predict the drag coefficient.

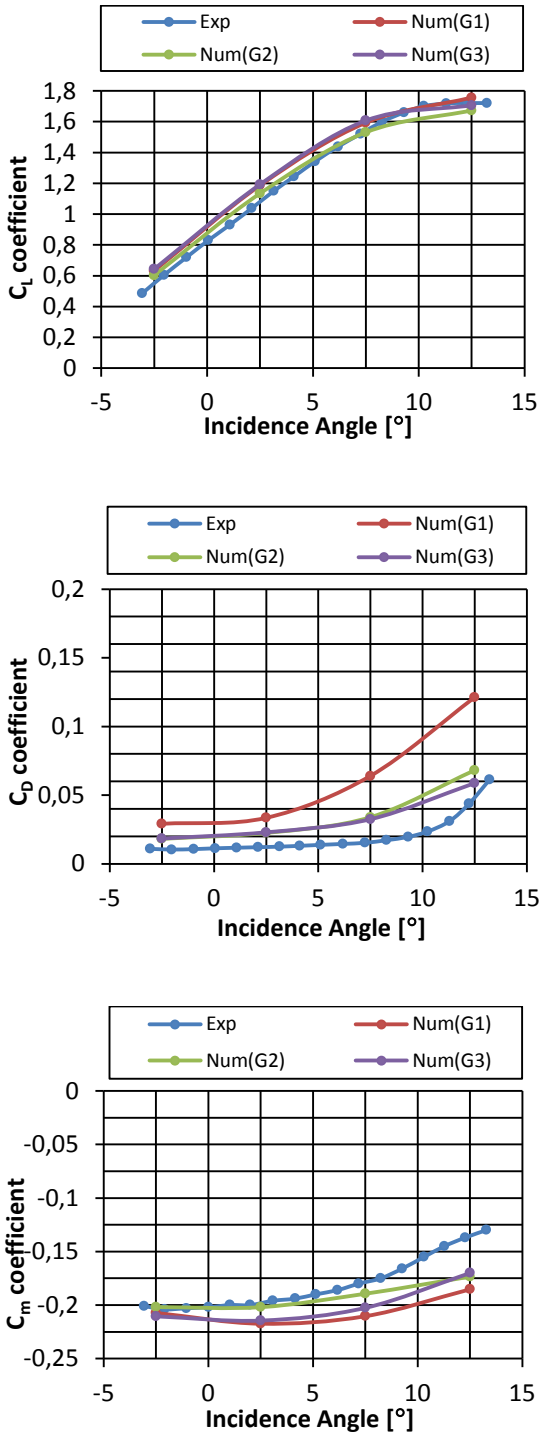


**Fig. 3.** Lift, drag and momentum coefficients for Spalart-Allmaras model.

For the momentum coefficient, a good accurate prediction of the values is shown, especially at low angles of attack .

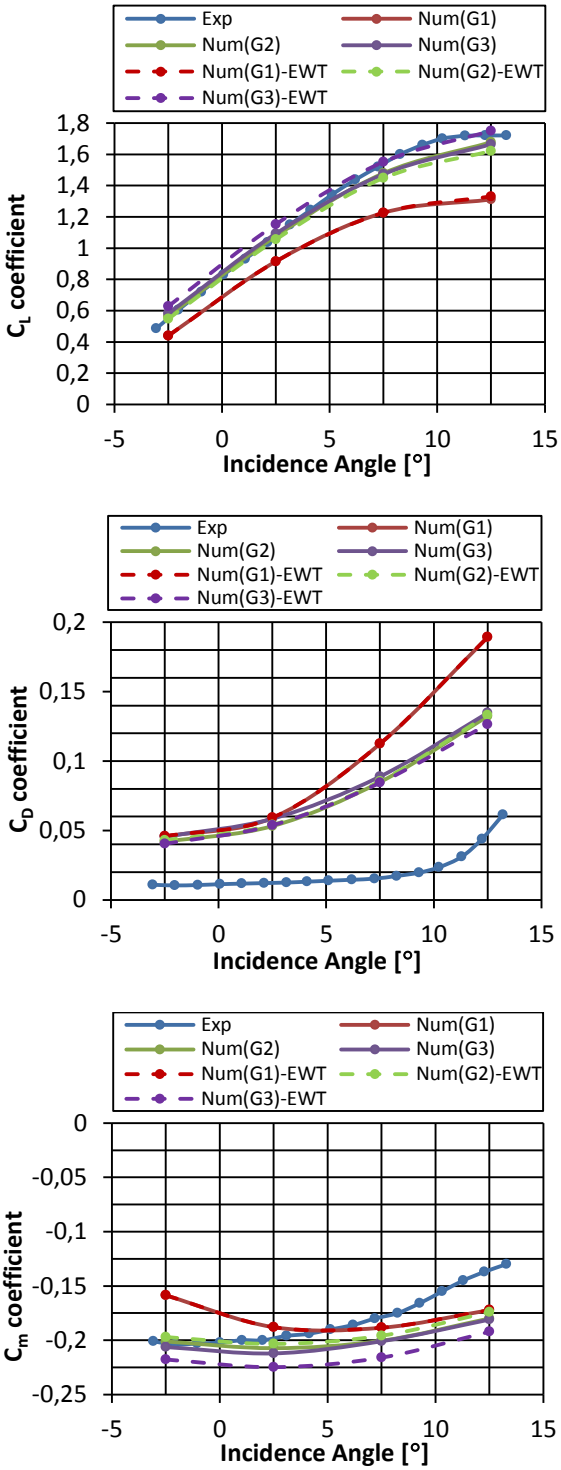


**Fig. 4.** Lift,drag and momentum coefficients for k-ε model.

*3.3. K-ω turbulence model*

In this turbulence model only the SST version is shown, because it is the model which has presented the best results, except for the middle mesh (G2), where the standard model had slightly better results with respect to the drag coefficient. The standard model has shown to reproduce the experimental curve with a good accuracy, except for high angles of attack in the finest meshes.

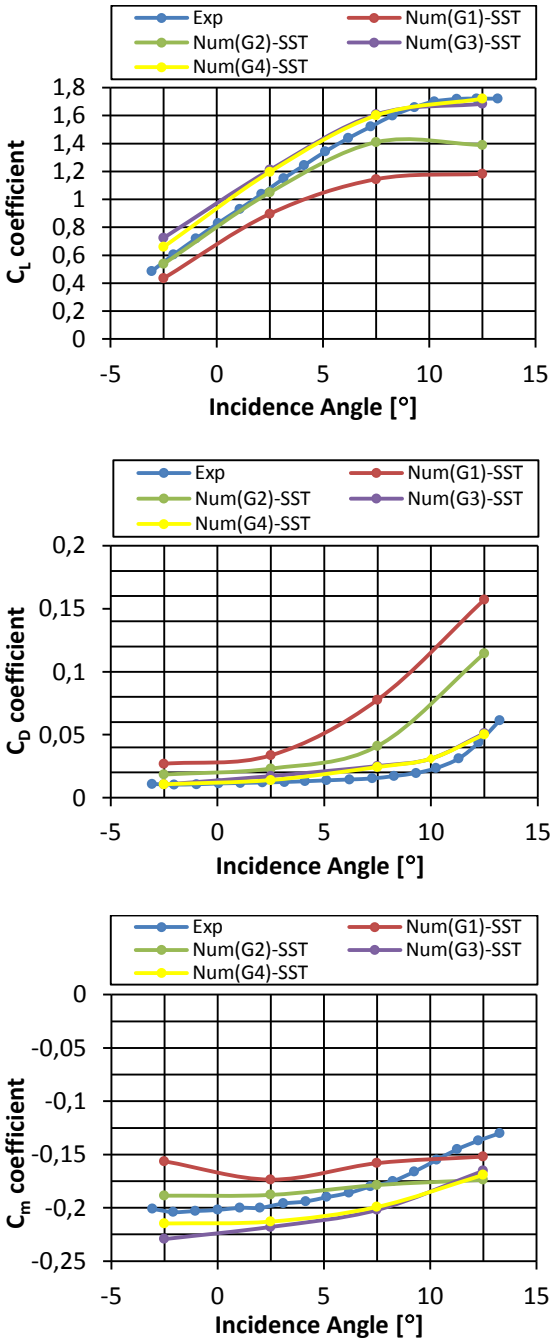


**Fig. 5.** Lift,drag and momentum coefficients for the k-ω SST model.

Looking at the lift coefficient chart, shown in Fig. 5, it can be noticed that in the most refined mesh exists a large accuracy at high angles, although the coefficient is over predicted for the lowest angles. In this case, the middle mesh (G2) is the one showing the best agreement with the experimental data.

In the graph of the drag coefficient, for the finest meshes, the numerical curve presents the highest accuracy with respect to the experimental one of the entire numerical database.

Finally, the momentum coefficient has an accurate prediction of values and tendencies; quite similar with the experimental curve, especially for the finest meshing (G4).

*3.4 Average unitary errors.*

Summary tables of average unitary errors for each turbulence model and for each mesh size are presented in this section. The computational time for each simulation is also shown.

These results show that refined meshes and complex turbulence models are not required for the lift coefficient. To obtain an accurate approximation, just a mesh with a relatively low number of cells (G2) and with a one-equation model as the Spalart-Allmaras can be used. Nevertheless, for the drag coefficient, it is very difficult to obtain accurate numerical results concerning experimental ones. A more complex turbulence model, such as k-ω SST, and high density meshes are required to achieve an acceptable error. Results for the momentum coefficient are better for k-ω standard model with a relatively refined mesh (G3), although low errors are also obtained for middle meshes and with a one equation turbulence model.

**Table 2.** Average unitary errors for the Spalart-Allmaras model.

| Spalart-Allmaras | | | | |
|---|---|---|---|---|
| **Tested Grids** | **Max. Computation times** | **Average unitary errors** | | |
| | | **$C_L$** | **$C_D$** | **$C_m$** |
| **G1** | 10 seconds | 0.08 | 1.93 | 0.18 |
| **G2** | 2 minutes | 0.03 | 0.73 | 0.10 |
| **G3** | 2 hours | 0.08 | 0.68 | 0.14 |

**Table 3.** Average unitary errors for the k-ε model with SWT.

| K-ε Standard Wall Function | | | | |
|---|---|---|---|---|
| **Tested Grids** | **Max. Computation times** | **Average unitary errors** | | |
| | | $C_L$ | $C_D$ | $C_m$ |
| **G1** | 10 seconds | 0.19 | 3.92 | 0.16 |
| **G2** | 1.5 minutes | 0.02 | 3.01 | 0.14 |
| **G3** | 2.5 hours | 0.03 | 3.28 | 0.15 |

**Table 4.** Average unitary errors for the k-ε model with EWT.

| K-ε Enhanced Wall Treatment | | | | |
|---|---|---|---|---|
| **Tested Grids** | **Max. Computation times** | **Average unitary errors** | | |
| | | $C_L$ | $C_D$ | $C_m$ |
| **G1** | 10 seconds | 0.19 | 3.93 | 0.16 |
| **G2** | 1.5 minutes | 0.03 | 3.07 | 0.12 |
| **G3** | 2.5 hours | 0.06 | 2.96 | 0.22 |

**Table 5.** Average unitary errors for the k-ω standard model.

| K-ω Standard | | | | |
|---|---|---|---|---|
| **Tested Grids** | **Max. Computation times** | **Average unitary errors** | | |
| | | $C_L$ | $C_D$ | $C_m$ |
| **G1** | 45 seconds | 0.22 | 2.50 | 0.17 |
| **G2** | 5 minutes | 0.07 | 0.95 | 0.08 |
| **G3** | 2.5 hours | 0.09 | 0.53 | 0.07 |
| **G4** | 2.75 hours | 0.06 | 0.55 | 0.06 |

**Table 6.** Average unitary errors for the k-Ω SST model.

| K-ω SST | | | | |
|---|---|---|---|---|
| **Tested Grids** | **Max. Computation times** | **Average unitary errors** | | |
| | | $C_L$ | $C_D$ | $C_m$ |
| **G1** | 45 seconds | 0.23 | 2.27 | 0.15 |
| **G2** | 5 minutes | 0.08 | 1.08 | 0.11 |
| **G3** | 2 hours | 0.12 | 0.27 | 0.16 |
| **G4** | 4 hours | 0.09 | 0.19 | 0.14 |

## 4. Conclusions

2D-RANS numerical models are able to predict global performance of wind turbine airfoils with reasonable accuracy and computation times of few hours (maximum) running in a conventional desktop personal computer.

Lift and momentum coefficients are accurately predicted with a simple one-equation Spalart-Allmaras turbulence model using medium meshes and computational times of a few minutes, for all the incidence angles tested. In these conditions, the numerical results for drag coefficient reproduce the global tendency of the experimental ones, but unitary errors are excessively high.

Drag coefficient is accurately predicted for all the incidence angles tested using the k-ω SST turbulence model with an adequate refined mesh, resulting in computational times of some hours. In these conditions, the results for lift and momentum coefficients are also accurate.

Global tendencies of lift, drag and momentum coefficients are well captured with these relatively simple models, thus allowing the comparison of alternative airfoil geometries in the design stage.


## Acknowledgement

This work has been supported by Project "Caracterización y predicción de la generación aerodinámica de ruido en perfiles de turbinas eólicas", DPI2011-25419. Ministerio de Economía y Competitividad, España.


## References


[1] Yu, G.H.; Zhu, X.C.; Du, Z.H., 2010, "Numerical simulation of a wind turbine airfoil: dynamic stall and comparison with experiments", Proceedings of the Institution of Mechanical Engineers, Part A: Journal of Power and Energy, Vol. 224, 657-677.

[2] Sorensen, N.N.; Michelsen, J.A., 2004, "Drag Prediction for Blades at High Angle of Attack Using CFD", Journal of Solar Energy Engineering, Vol. 126, 1011-1016.

[3] Fleig, O.; Iida, M.; Arakawa, C., 2004, "Wind Turbine Blade Tip Flow and Noise Prediction by Large-eddy Simulation", Journal of Solar Energy Engineering, Vol. 126, 1017-1024.

[4] Selig, M.S.; McGranahan, B.D., 2004, "Wind Tunnel Aerodynamic Tests of Six Airfoils for Use on Small Wind Turbines", NREL/SR-500-34515.